

Non-linear interplay between edge localized infernal mode and plasma flow

G. Q. Dong,¹ Y. Q. Liu,^{2,1} Y. Liu,¹ S. Wang,¹ N. Zhang,¹ G. Z. Hao,¹ and G. L. Xia¹

¹Southwestern Institute of Physics, Post Office Box 432, Chengdu 610041, China

²General Atomics, PO Box 85608, San Diego, California 92186-5608, USA

*E-mail contact of main author: donggq@swip.ac.cn; liuy@fusion.gat.com

Quiescent H-mode (QH-mode) was first discovered in DIII-D as an ELM-free H-mode regime, which is usually achieved at relatively low plasma density and found to be accompanied by the presence of edge harmonic oscillations (EHOs).^[1-4] EHOs are believed to provide necessary transport to eliminate ELMs by dynamics of the plasma itself. The saturated kink-peeling mode has been suggested as a possible candidate for EHO.^[5] In this work, we consider another instability – the edge localized infernal mode (ELIM) – as a possible candidate, for plasmas where the large edge bootstrap current causes local flattening of the plasma edge safety factor, or even the magnetic shear reversal in the pedestal region. An ELIM is a low- n (n is the toroidal mode number) instability similar to the conventional infernal mode, but being localized at the plasma edge where safety factor is locally flattened. Finite plasma pressure in the pedestal region drives this mode. A saturated ELIM, due to non-linear interaction with toroidal plasma edge flow, can be responsible for EHO.

Our investigation is divided into three stages: (i) linear stability, or the ELIM onset condition, at a given plasma flow; (ii) comparison of various toroidal torques, generated by a linear mode instability; (iii) non-linear interplay between an ELIM and the toroidal plasma flow.

A systematic numerical investigation, utilizing the free boundary MARS-F/K codes^{[6][7]}, shows that both plasma resistivity and toroidal flow shear destabilize the ELIM. The drift kinetic effects, due to mode resonance with precessional and bounce motions of trapped thermal particles, are found to be stabilizing for the mode, albeit not dramatic^[8]. The mode eigen-structure, with one example shown in Fig. 1(a), on the other hand, is sufficiently rigid against the variation of the plasma flow or resistivity, or the drift kinetic effects.

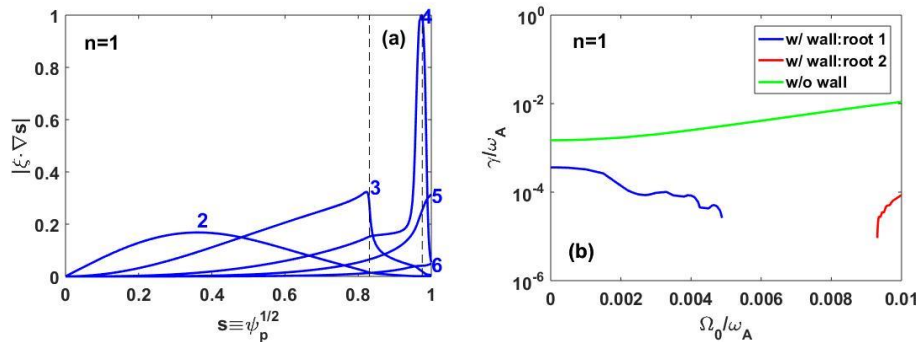


FIG. 1. (a) The typical eigen-structure of the computed $n=1$ ELIM instability, with the dominant $m=4$ poloidal Fourier harmonic peaking at the local minimum of the safety factor q near the plasma edge ($s \approx 0.98$ in this case where the $q=4$ surface is located). (b) The growth rate γ versus the on-axis rotation

frequency of a sheared toroidal flow of the plasma, with or without a close-fitting resistive wall.

We also find that the low- n ELIM instability is strongly affected by a close-fitting resistive wall. The presence of a resistive wall can fully stabilize an otherwise flow-shear destabilized ELIM. One example of the $n=1$ linear ELIM is shown in Fig. 1(b), for a circular shaped toroidal plasma of minor radius a , and with a resistive wall being placed at $1.1a$. A stability window opens by the combined effects of the plasma flow and the resistive wall. Two unstable roots, of different characteristics, are computed outside the stable window. One root (root 1, at slow rotation) rotates with the plasma, whilst the other (root 2, at fast flow) is locked to the wall (similar to the resistive wall mode).

The ELIM instability, like many other MHD instabilities, generates toroidal torques which in turn can affect the plasma flow. For a linear ELIM perturbation (at a given rotation), we compute and compare the resulting three types of toroidal torques: the resonant electromagnetic ($\mathbf{j} \times \mathbf{b}$) torque, the toroidal torques due to Reynolds stress and neoclassical toroidal viscosity (NTV). We find that both $\mathbf{j} \times \mathbf{b}$ and Reynolds stress torques, associated with root 1, are highly localized near mode rational surfaces. The NTV torque is more global. The Reynolds stress torque provides the largest local torque near the plasma edge.

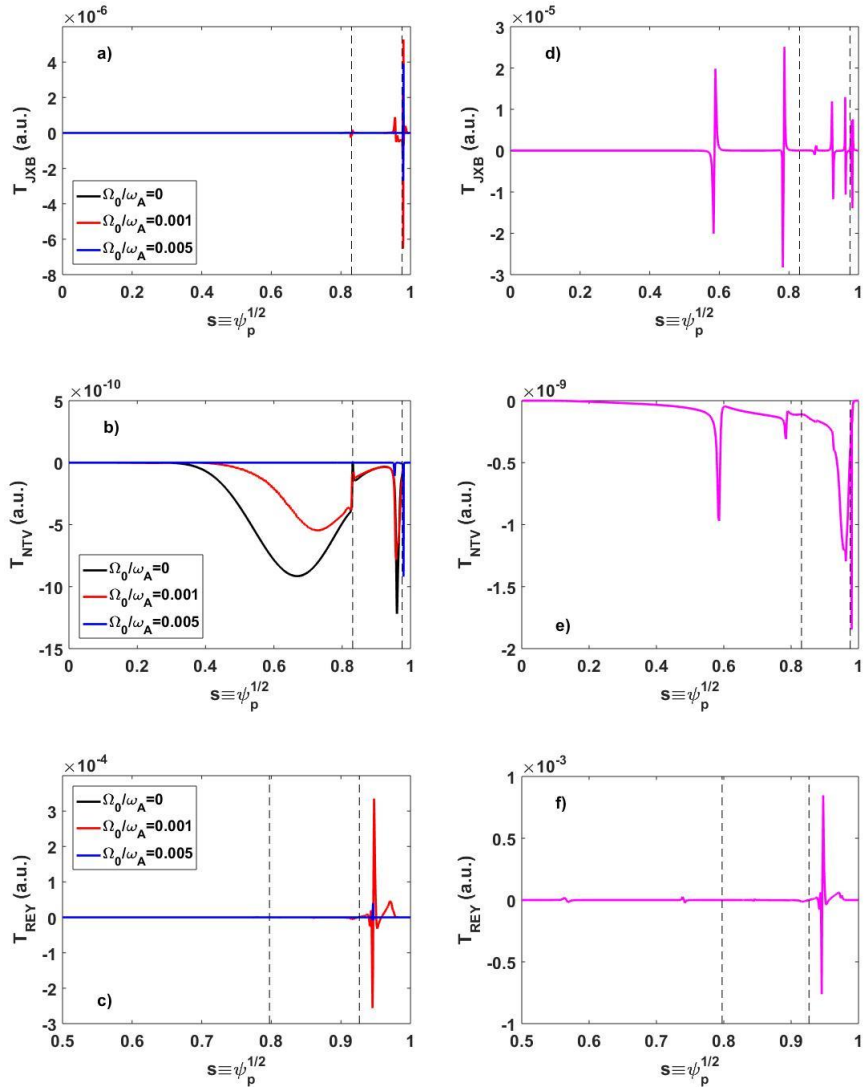


FIG. 2. Radial profiles of the computed toroidal torque densities, assuming eigenfunctions associated with root 1 (left panels) and root 2 (right panels), for (a, d) the toroidal electromagnetic $\mathbf{j} \times \mathbf{b}$ torque, (b, e) the NTV torque, and (c, f) the Reynolds stress torque. A fixed shear flow profile (shown in Fig. 3) is assumed. The dashed vertical lines indicate radial locations of the $q=3$ and $q=4$ rational surfaces, respectively.

An interesting observation is the presence of multiple peaks off rational surfaces (Fig. 2(d,e)), in the computed torque density profiles associated with root 2 at finite flow ($\Omega_0/\omega_A = 0.01$). These peaks, being numerically well resolved, are due to the so called resonant splitting effect^[9], which occurs when the ELIM rotates in the plasma frame (i.e. for root 2 which has nearly vanishing real frequency in the laboratory frame). In this case, the mode is subject to continuum resonances with the shear Alfvén waves and the sound wave, as illustrated by Fig. 3.

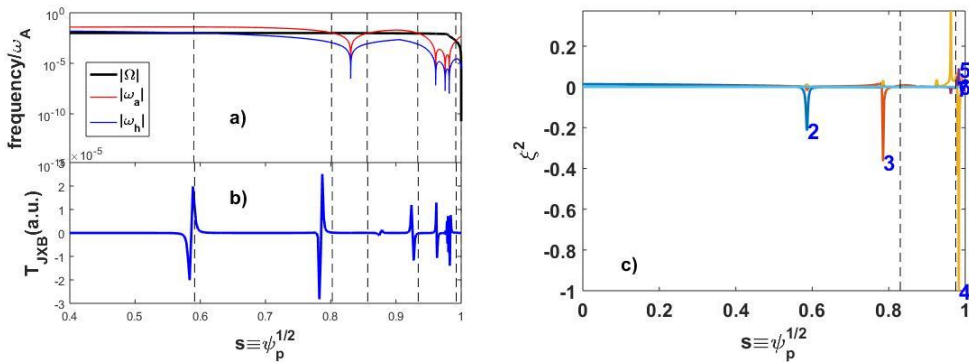


FIG. 3. (a) Radial profiles of the sheared plasma rotation frequency $|\Omega|$, the analytic expressions for the shear Alfvén frequency $|\omega_a|$ and the sound frequency $|\omega_h|$, plotted as a function of the minor radius. (b) The radial distribution of the computed electromagnetic torque density. (c) The radial distribution of the poloidal displacement for ELIM. The dashed line in (a) and (b) indicates the resonant surface between the latter two frequency and the plasma rotation frequency, while the dashed line in (c) denotes the rational surface.

Continuum resonances also produce finite plasma displacement at the splitted resonant surfaces. Figure 3 (c) shows one example for the poloidal component of the computed plasma displacement. Since the Reynolds stress torque is roughly proportional to the square of the plasma displacement. The radial distribution of the torque density also exhibits the resonant splitting effect (Fig. 2(e)).

Next, we investigate the non-linear interplay between the ELIM and the plasma flow, by performing initial value simulations with the quasi-linear code MARS-Q^[10]. We start simulations at a prescribed rotation speed. Three initial conditions are considered, representing three typical situations shown in Fig. 1(b): (i) with a resistive wall and starting with root 1 at on-axis toroidal rotation frequency of $0.005\omega_A$ (ω_A is toroidal Alfvén frequency); (ii) with a resistive wall and starting with root 2 at on-axis rotation of $0.01\omega_A$; (iii) without resistive wall and starting an on-axis rotation of $0.005\omega_A$. The eventual goal of these simulations is to achieve a good understanding of how the ELIM can affect the local flow shear, and how the change of the local flow shear can in turn modify the ELIM instability. One result is reported in Fig. 4, for case (iii). Compared in Fig. 4(a) are time traces of the amplitude of two resonant field

harmonics near the plasma edge. These field perturbations illustrate the mode instability. Compared to the linear runs, where the mode linearly grows (dashed lines), the quasi-linear run shows partial saturation of the mode. Meanwhile, the toroidal rotation profile (Fig. 4(b)), especially that near the plasma edge where the mode is located, is significantly reduced, together with the local flow shear near the $q=4$ surface. It is this reduction of the local flow shear that leads to the eventual mode saturation in this simulation.

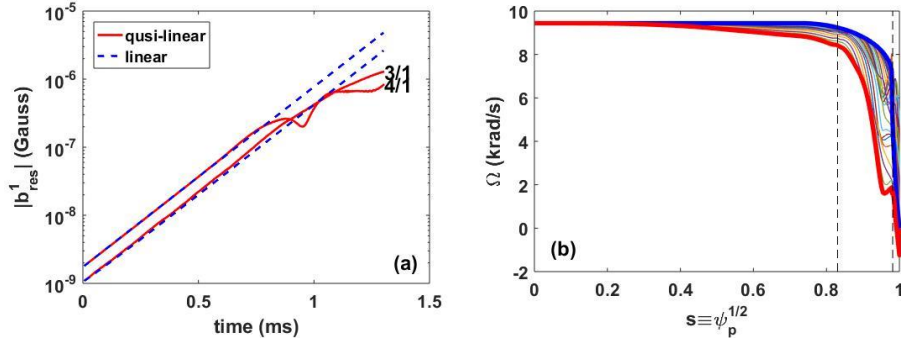


FIG. 4. Quasi-linear initial value simulations of a linearly unstable $n=1$ ELIM: (a) amplitude of the perturbed resonant radial field b^1 at the $q=3$ and $q=4$ surfaces and (b) evolution of the radial profile of the plasma rotation due to non-linear interplay with the ELIM, with the initial rotation in thick blue, which evolves into the thick red curve after 1.3 ms. Dashed lines in (a) indicate linear mode growth at fixed (initial) rotation. Vertical dashed lines in (b) indicate the location of the $q=3$ and $q=4$ surfaces, respectively. No resistive wall is present in the simulations.

In Summary, MARS-F linear stability computations show that, in the absence of a resistive wall, the plasma edge flow shear destabilizes the edge localized infernal mode. However, the presence of a close-fitting resistive wall opens up a stability window, as the plasma rotation frequency increases. The two unstable roots outside the stability window exhibit different characteristics, especially in terms of the real frequency of the mode. The non-rotating mode, in the plasma frame, produces toroidal torque densities that peak off rational surfaces, due to resonant splitting effect associated with shear Alfvén and sound waves. Quasi-linear simulations with MARS-Q demonstrate ELIM mode saturation, accompanied by the local flow (and flow shear) reduction near the plasma edge.

References

- [1] K. Burrell, *et al*, Phys. Plasmas **12**, 056121 (2005)
- [2] K. Burrell, *et al*, Phys. Plasmas **8**, 2153 (2001)
- [3] K. H. Burrell, *et al*, Plasma Phys. Controlled Fusion **44**, A253 (2002)
- [4] W. Suttrop, *et al*, Plasma Phys. Controlled Fusion **45**, 1399 (2003)
- [5] X. Chen, *et al*, Nucl. Fusion **56**, 076011 (2016)
- [6] Y. Q. Liu, *et al*, Phys. Plasmas **7**, 3681 (2000).
- [7] Y. Q. Liu, *et al*, Phys. Plasmas **15**, 112503 (2008).
- [8] G. Q. Dong, *et al*, Physics of Plasmas **24**, 112510 (2017).
- [9] Y.Q. Liu, *et al*, Phys. Plasmas **19**, 102507 (2012)
- [10] Y. Q. Liu, *et al*, Phys. Plasmas **20**, 042503 (2013).